

# Mechanistic Studies of Methane Biogenesis by Methyl-Coenzyme M Reductase: Evidence that Coenzyme B Participates in Cleaving the C–S Bond of Methyl-Coenzyme M<sup>†</sup>

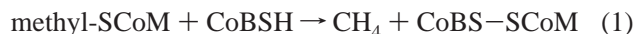
Yih-Chern Horng, Donald F. Becker,<sup>§</sup> and Stephen W. Ragsdale\*

Department of Biochemistry, Beadle Center, University of Nebraska, Lincoln, Nebraska 68588-0664

Received June 11, 2001; Revised Manuscript Received August 14, 2001

**ABSTRACT:** Methyl-coenzyme M reductase (MCR), the key enzyme in methanogenesis, catalyzes methane formation from methyl-coenzyme M (methyl-SCoM) and *N*-7-mercaptoheptanoylthreonine phosphate (CoBSH). Steady-state and presteady-state kinetics have been used to test two mechanistic models that contrast in the role of CoBSH in the MCR-catalyzed reaction. In class 1 mechanisms, CoBSH is integrally involved in methane formation and in C–S (methyl-SCoM) bond cleavage. On the other hand, in class 2 mechanisms, methane is formed in the absence of CoBSH, which functions to regenerate active MCR after methane is released. Steady-state kinetic studies are most consistent with a ternary complex mechanism in which CoBSH binds before methane is formed, as found earlier [Bonacker et al. (1993) *Eur. J. Biochem.* 217, 587–595]. Presteady-state kinetic experiments at high MCR concentrations are complicated by the presence of tightly bound CoBSH in the purified enzyme. Chemical quench studies in which <sup>14</sup>CH<sub>3</sub>-SCoM is rapidly reacted with active MCRred1 in the presence versus the absence of added CoBSH indicate that CoBSH is required for a single-turnover of methyl-SCoM to methane. Similar single turnover studies using a CoBSH analogue leads to the same conclusion. The results are consistent with class 1 mechanisms in which CoBSH is integrally involved in methane formation and in C–S (methyl-SCoM) bond cleavage and are inconsistent with class 2 mechanisms in which CoBSH binds after methane is formed. These are the first reported pre-steady-state kinetic studies of MCR.

One billion tons of the greenhouse gas methane are generated annually. Methyl-coenzyme M reductase (MCR)<sup>1</sup> catalyzes the final step in methane formation from methyl-coenzyme M (methyl-SCoM) and *N*-7-mercaptoheptanoylthreonine phosphate (CoBSH) (eq 1) (1). CoBSH serves as the electron donor (2) and the mixed disulfide CoBS-SCoM is the product of the reaction. Central to catalysis is a nickel tetrapyrrole cofactor called Factor F<sub>430</sub> (3–5), which is active in a Ni(I) state called MCR<sub>red1</sub> (6). It appears certain that the Ni(I) state of F<sub>430</sub> is required to initiate catalysis (6–8) since there is a direct correlation between Ni(I) (MCR<sub>red1</sub>) formation and MCR activity in *Methanobacterium thermoautotrophicum* (6) and *Methanosarcina thermophila* (9). It is proposed that the methyl group of methyl-SCoM, possibly complexed with CoBSH (see below), suffers nucleophilic attack by Ni(I) to form a methyl-Ni species, which undergoes protonolysis to form methane (10).



Steady-state kinetic (11, 12) and crystallographic studies (13) support an ordered mechanism in which first methyl-SCoM and then CoBSH bind, followed by formation of methyl-Ni and CoBS-SCoM (see ref 10 for review). Factor F<sub>430</sub> forms the base of a narrow well that neatly accommodates the two substrates. CoBSH binds at the top of the well with its phosphate group at the upper lip and its thiol about 6 Å from the Ni site of F<sub>430</sub>. In the “ox1-silent” state, which may mimic the early stages of the reaction, the sulfur of HSCoM binds near the base of the well as the upper axial nickel ligand. Cryoreduction experiments indicate that the EPR-active “ox1” state has a similar coordination environment as ox1-silent (14). In the Ni(II)-silent state, the product of the reaction CoB-SS-CoM is in the active site with the “CoBS” moiety in the same location, but with “CoMS” ligated to the sulfonate through the sulfonate oxygens. Thus, SCoM or methyl-SCoM can exist in two alternate orientations in the active site. The active “red1” is similar to the Ni(II)-silent state in containing either a weak upper axial sulfonate ligand or possibly an open upper axial site (14). EPR, ENDOR, and cryoreduction experiments indicate that the ox1 and red1 states contain Ni(I) (14, 15).

What is the role(s) of CoBSH in this reaction? Two classes of mechanisms for methane biogenesis by MCR (10) are summarized in Figure 1. These can be distinguished by whether CoBSH is required for cleavage of the C–S bond of methyl-SCoM. In mechanistic class 1, CoBSH is involved

<sup>†</sup> This work was supported by Department of Energy Grant ER-20053 (S.W.R.).

\* To whom correspondence should be addressed. Department of Biochemistry, Beadle Center, University of Nebraska, Lincoln, NE 68588-0664, Phone: 402-472-2943. Fax: 402-472-8912. E-mail: sragdale1@unl.edu.

<sup>§</sup> Present address: Chemistry Department, University of Missouri-St. Louis, 319 Benton Hall, 8001 Natural Bridge Road, St. Louis, MO 63121.

<sup>1</sup> MCR, methyl-coenzyme M reductase; methyl-SCoM, methyl-coenzyme M; CoBSH, *N*-7-mercaptoheptanoylthreonine phosphate or coenzyme B; CoBS-SCoM, the heterodisulfide product of the MCR reaction.

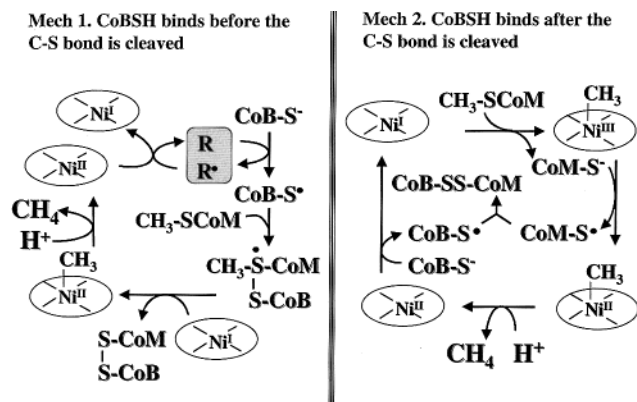


FIGURE 1: Two mechanistic classes for the MCR reaction. In mechanistic class 1, CoBSH is involved directly in C–S bond cleavage, similar to the Berkessel mechanism (17). “R” is a possible radical species that is responsible for oxidation of CoBSH to a radical; possibly this is the thioglycine/thioethyl radical couple. In the class 2 mechanism, the C–S bond is cleaved before CoBSH reacts. See text for details.

directly in C–S bond cleavage. The R• reflects an active site radical species. Possibly it reflects a thiocetyl radical, which has been suggested to play a role in the MCR reaction (16). A methylsulfuranyl radical species is shown to be the direct precursor of the methyl-Ni intermediate, as proposed by Berkessel (17). On the other hand, in the class 2 mechanism, the C–S bond is cleaved before CoBSH reacts. In this specific example, CoBSH serves only as an electron donor involved in reducing Ni(II) back to the active Ni(I) state. In both mechanisms, a methyl-Ni intermediate is proposed to undergo protonolysis to form methane. These mechanistic schemes are presented to contrast whether CoBSH is involved in cleaving the C–S bond of methyl-SCoM and other mechanisms involving different intermediates could be imagined for either the class 1 or 2 mechanism. The steady-state and crystallographic experiments described above appear most consistent with the class 1 mechanism; however, the limitations of steady-state kinetics warrant investigations by transient kinetics approaches. Either mechanism would be consistent with stereochemical studies in which a net inversion of configuration is observed when ethyl-SCoM is reduced to ethane (18). The inversion is expected to occur when the methyl-Ni intermediate is formed, whereas the subsequent protonolysis should proceed with retention of configuration, resulting in net inversion.

The purpose of this investigation, which represents the first reported transient kinetic study of MCR, is to narrow the choices to class 1 or class 2 mechanisms. These mechanisms can be distinguished by determining whether the C–S bond is cleaved in the absence of CoBSH in a single turnover reaction. In the class 1 mechanism, a single turnover of methane formation requires CoBSH; in contrast, the class 2 mechanism predicts that the first turnover of methane can occur in the absence of CoBSH. We have used a rapid chemical quench approach in which <sup>14</sup>C-methyl-SCoM is reacted with the active MCR<sub>red</sub> state in the presence and absence of CoBSH, and the reaction mixture is rapidly quenched with acid. Our results indicate that CoBSH is required for methane formation in a single turnover reaction, suggesting that CoBSH is integrally involved in the steps leading up to C–S bond cleavage.

## MATERIALS AND METHODS

**Materials.** *Methanothermobacter marburgensis* (f. *M. thermoautotrophicum* strain Marburg) was obtained from the Oregon Collection of Methanogens catalogued as OCM82. Sodium sulfide was purchased from Sigma. Monobromobimane (Thiolite) was purchased from Novabiochem. All buffers, media ingredients, and other reagents were acquired from Sigma. Solutions were prepared using Nanopure deionized water. N<sub>2</sub> (99.98%), N<sub>2</sub>/H<sub>2</sub> (90%/10%), Ar (99.8%), H<sub>2</sub>/CO<sub>2</sub> (80%/20%), and CH<sub>4</sub>/N<sub>2</sub> (0.2%/99.8%) were obtained from Linwood (Lincoln, NE).

Methyl-SCoM and <sup>14</sup>C-labeled methyl-SCoM were prepared from coenzyme M (Sigma) and methyl iodide (Sigma) and <sup>14</sup>C-labeled methyl iodide (Amersham), respectively (19). After methyl-SCoM was crystallized twice in acetone, its purity was checked by <sup>1</sup>H NMR. The purity of <sup>14</sup>C-labeled methyl-SCoM was evaluated by comparing the MCR activity under nonsaturating conditions using <sup>14</sup>C-labeled methyl-SCoM with that using methyl-SCoM. CoBS-SCoB was prepared as described from 7-bromoheptanoic acid (Karl Industries), 6-bromocaproic acid (Fluka), N-hydroxysuccinimide (Sigma-Aldrich), and *o*-threonine-phosphate (Sigma-Aldrich) (20–22). Synthesis of the 6-carbon analogue, CoB<sub>6</sub>S-SCoB<sub>6</sub>, was performed following the same steps as for CoBS-SCoB. CoBS-SCoB and CoB<sub>6</sub>S-SCoB<sub>6</sub> were purified on a preparative C<sub>18</sub> column (3.4 × 4 cm) (Waters, No. 51922) equilibrated with 50 mM (NH<sub>4</sub>)<sub>2</sub>CO<sub>3</sub> (pH 3.3). The threonine phosphate and the hydroxyl succinimide produced in the reaction were eluted with 20% methanol in 50 mM (NH<sub>4</sub>)<sub>2</sub>CO<sub>3</sub> (pH 3.3). The fractions that eluted in 80% methanol contained only CoBS-SCoB (or CoB<sub>6</sub>S-SCoB<sub>6</sub>) as analyzed by <sup>1</sup>H NMR and HPLC. These fractions were lyophilized and the product was stored at –20 °C. CoBSH (or CoB<sub>6</sub>SH) was generated from CoBS-SCoB (CoB<sub>6</sub>S-SCoB<sub>6</sub>) by anaerobic reduction with NaBH<sub>4</sub> (11). After acidification with HCl to a pH below 1.0, the reaction mixture was applied to a preparative C<sub>18</sub> column (2 × 5 cm) equilibrated with anaerobic 50 mM (NH<sub>4</sub>)<sub>2</sub>CO<sub>3</sub> (pH 3.3). After the column was washed with this buffer to remove salts, CoBSH was eluted with 60% methanol in 50 mM (NH<sub>4</sub>)<sub>2</sub>CO<sub>3</sub> (pH 3.3). The fractions containing CoBSH (or CoB<sub>6</sub>SH) were identified with Ellman's reagent and were pooled and lyophilized. The purity of CoBSH (or CoB<sub>6</sub>SH) was ascertained by HPLC. The concentration of CoBSH was checked routinely with Ellman's reagent before using.

CoBS-SSCoB, CoB<sub>6</sub>S-SCoB<sub>6</sub>, CoBSH, and CoB<sub>6</sub>SH concentrations were determined by HPLC and monitored by following their absorbance at 207 nm. The column (Phenomenex Spherex 10 μ C<sub>18</sub>, 250 × 4.60 mm) was pre-equilibrated with 50 mM (NH<sub>4</sub>)<sub>2</sub>CO<sub>3</sub> (pH 3.3) and eluted in a 30 min gradient from 0 to 100% methanol at a flow rate of 1 mL/min. The retention times for CoBS-SCoB, CoB<sub>6</sub>S-SCoB<sub>6</sub>, CoBSH, CoB<sub>6</sub>SH were 23, 21, 16, and 11 min, respectively.

Ti(III) citrate solutions were prepared from a stock solution of 200 mM Ti(III) citrate, which was made by dissolving 0.75 g of Ti(III) trichloride (Fluka) in 25 mL of 250 mM sodium citrate (Sigma) under anaerobic conditions and then adjusting the pH to 7.0 with sodium bicarbonate (Sigma). The concentration of reducing equivalents of Ti(III) was determined by titrating a benzyl viologen solution.

**Mt. marburgensis Growth, Harvest, and Purification Conditions.** *Mt. marburgensis* was cultured on  $\text{H}_2/\text{CO}_2/\text{H}_2\text{S}$  (80%/20%/0.1%) at 65 °C in a 14-L New Brunswick fermentor (6, 23). Media was prepared as previously described (23). Once the culture had reached late log phase ( $A_{578} \sim 3.0$ ), sodium sulfide was added directly to the growing cells (final sulfide concentration, 20 mM) prior to harvesting as described (9). After 15 min at 65 °C, the culture was cooled to 25 °C within 30 min and harvested anaerobically.

$\text{MCR}_{\text{ox1}}$  was purified as described except that methyl-SCoM was omitted from the lysis buffer (6). For experiments requiring high concentrations of MCR,  $\text{MCR}_{\text{ox1}}$  was concentrated under argon (that had been passed through an oxisorb column to remove oxygen) pressure in a 10-mL omegacell (Filtron) with a 30 kDa molecular mass cutoff.

**MCR Activation.**  $\text{MCR}_{\text{ox1}}$  was activated to the red1 state in the presence of methyl-SCoM in a reaction mixture including 20 mM Ti(III) citrate, 10 mM methyl-SCoM, 0.67 M TAPS (pH 10), 16.7 mM Tris-Cl (pH 7.6), and MCR (30 to 200  $\mu\text{M}$ ). The mixture was heated at 60 °C for 30 min, cooled on ice, and neutralized to pH 7.0–7.1 by adding an equal volume of 2 M MOPS (pH 7.0) (6). Activation of  $\text{MCR}_{\text{ox1}}$  without methyl-SCoM was similar except that methyl-SCoM was excluded from the mixture and the heating at 60 °C was extended to 40 min, which maximized Ni(I) formation and specific activity under these conditions. Protein concentrations were determined by the Bradford method using the Bio-Rad reagent (Bio-Rad) and bovine serum albumin as a standard (24).  $F_{430}$  content was estimated by using the extinction coefficient of 22 000  $\text{cm}^{-1} \text{M}^{-1}$  at 420 nm (25).

**Measurement of MCR Activity.** MCR assays were performed at 65 °C in rubber-sealed 8-mL serum vials. The standard assay mixture contained 20 mM methyl-SCoM, 1.2 mM CoBSH, 0.6 mM aquocobalamin, 25 mM Ti(III)citrate, and 0.5 M MOPS (pH 7.0) in a final volume of 0.4 mL. The reaction was started by increasing the temperature from 4 to 65 °C. Methane generated by MCR during the assay was determined by withdrawing gas samples at specific time points for analysis by gas chromatography (Varian model 3700 equipped with a flame ionization detector). Rates of methane formation were then calculated from the linear portion of the time course. One unit of MCR activity is equal to 1  $\mu\text{mol}$  of methane  $\text{min}^{-1}$ .

**Spectroscopy of MCR.** UV–visible spectra of MCR were recorded with a diode array spectrophotometer (Beckman series 7000). EPR spectra were recorded on a Bruker ESP 300E spectrometer equipped with an Oxford ITC4 temperature controller, a Hewlett-Packard model 5340 automatic frequency counter and Bruker gaussmeter. The EPR spectroscopic parameters for quantifying the  $\text{MCR}_{\text{ox1}}$  and  $\text{MCR}_{\text{red1}}$  EPR signals were the following: temperature, 120 K; microwave power, 10 mW; microwave frequency, 9.43 GHz; receiver gain,  $2 \times 10^4$ ; modulation amplitude, 12.8 G; modulation frequency, 100 kHz. Double integrations of the EPR spectra were performed with copper perchlorate (1 mM) as the standard.

**Steady-State and Pre-Steady-State Kinetic Experiments.** To determine the dependence of MCR activity on CoBSH, MCR was activated in the absence of methyl-SCoM. For experiments performed under  $V_{\text{max}}/K_m$  conditions, methyl-

SCoM concentrations were maintained at 100  $\mu\text{M}$ , since the  $K_m$  for methyl-SCoM is 5.4 mM for the MCR 1 isoenzyme under the conditions used here. The assay mixture (1 mL volume) contained: 20 mM Ti(III) citrate, 0.5 M MOPS (pH 7.0), 0.1 mM methyl-SCoM, 0.3 mM hydroxocobalamin, and varying concentrations of CoBSH. The reaction was started by increasing the temperature from 4 to 65 °C. Methane generated during the assay was determined by withdrawing gas samples at specific time points for analysis by gas chromatography for up to 50 min. The  $V_{\text{max}}/K_m$  values were determined for each concentration of CoBSH by fitting the plot of product, methane ( $\mu\text{M}$ ), formation (eq 2) or substrate (methyl-SCoM) decay (eq 3) versus time (min) to a theoretical single-exponential equation.

$$[S] = S_0 \exp(-V/Kt) \quad (2)$$

$$[P] = [P_{\text{max}}](1 - \exp(-V/Kt)) \quad (3)$$

Chemical-quench experiments were performed using an Update Instruments chemical/freezing-quench apparatus with a model 745 controller. The temperature for the experiments was 20 °C. Rapid reaction kinetic studies were performed with  $\text{MCR}_{\text{red1}}$  and  $^{14}\text{CH}_3\text{-SCoM}$  in separate stopped-flow syringes (typically 2-mL syringes).  $\text{MCR}_{\text{red1}}$  was in buffer (final pH 7.0–7.1) containing 1 M MOPS (pH 7.0), 0.33 M TAPS (pH 10.0), and 1 mM Ti(III) citrate while  $^{14}\text{CH}_3\text{-SCoM}$  concentrations were prepared in 0.5 M MOPS (pH 7.0) with 0.5 mM Ti(III) citrate.

Rapid mixing of  $\text{MCR}_{\text{red1}}$  and  $^{14}\text{CH}_3\text{-SCoM}$  was achieved by displacing each syringe by 1 mm which generated a total reaction volume of 66  $\mu\text{L}$  (33  $\mu\text{L}$  from each syringe) per shot. The ram speed was varied from 0.8 to 8.0 cm/s and was shown not to affect the observed reaction rate. Typically, a ram speed of 6.4 cm/s was used with a 15 ms aging time. For each data point, four shots were collected (264  $\mu\text{L}$ ) in an 18-mL scintillation vial containing 0.2 mL of 2 N perchloric acid. The reaction was monitored by following the loss of  $^{14}\text{C}$  from the substrate. Data were fit to single- and double-exponential decay equations using Sigma Plot.

The activity of  $\text{MCR}_{\text{red1}}$  was measured prior to the rapid reaction kinetic experiments. The typical specific activity of the MCR used for the chemical quench studies was 20–25 U/mg at 65 °C, which would be equivalent to 60 to 100 U/mg, when corrected to 100% active  $\text{MCR}_{\text{red1}}$ . The amount of  $\text{MCR}_{\text{red1}}$  in each chemical quench experiment was measured by integrating the  $\text{MCR}_{\text{red1}}$  EPR signal. Quantitation of  $\text{MCR}_{\text{red1}}$  was performed before and after the chemical quench experiments. This allowed us to monitor the loss of  $\text{MCR}_{\text{red1}}$  during the experiment, which was less than 10% loss. The  $\text{MCR}_{\text{red1}}$  concentration determined after the chemical quench experiments were completed is the amount reported in the figure legends. Typical spin concentrations of the  $\text{MCR}_{\text{red1}}$  in the MCR samples for chemical quench ranged from 0.25 to 0.35 spin/mol of MCR.

**Determination of Methyl-SCoM and CoBSH in MCR.** Purified MCR (35  $\mu\text{M}$ ) was digested overnight with pepsin at 37 °C, in 5 mM ammonium formate (pH 3.3). After filtration of the MCR pepsin digest through a 1-kDa membrane, the filtrate was analyzed by mass spectrometry (negative ion mode). Absorbance measurements at 430 nm of the uncomplexed  $F_{430}$  in the filtrate showed 100% of the



F<sub>430</sub> was released from MCR during the digest, indicating that MCR (namely, the active site) had been completely denatured. Methyl-SCoM standards were prepared by making a series of methyl-SCoM concentrations (5 to 50  $\mu$ M) in 5 mM ammonium formate (pH 3.3).

We were unable to obtain reliable results with either our sample or with CoBSH standards using mass spectroscopy (positive and negative ion mode). Therefore, we determined CoBSH by HPLC methods either directly by monitoring the elution profile by its absorbance at 207 nm or as the monobromobimane adduct, as reported previously for HSCoM (11). Purified MCR (105 mg) was digested overnight with pepsin at 37 °C in 5 mM ammonium formate (pH 3.3). Complete digestion was evident by the release of F<sub>430</sub>. The digested protein was lyophilized and resuspended in 0.9 mL of water. For the monobromobimane adduct, in an anaerobic chamber, 0.3 mL of NaBH<sub>4</sub> (2 M in 50 mM NaOH) was added to the digested protein solution. To this solution of 1.2 mL, 0.15 mL of monobromobimane (20 mM in acetonitrile) was added. The reaction was allowed to run for 10–15 min and was then stopped by adding perchloric acid.

The mixture was analyzed by HPLC using a C-18 preparatory column and monitored using an absorbance detector. A 0–80% methanol gradient in 10 mM ammonium formate (pH 3.3) over 30 min eluted the CoBS-monobromobimane derivative at 28 min. The peak at 28 min was identified as CoBS-monobromobimane by comparing the elution profile with that of authentic CoBS-monobromobimane and by fluorescence spectroscopy. Quantitation of CoBSH in the MCR sample was achieved by relating the fluorescence of the CoB-monobromobimane samples to a CoBS-monobromobimane standard curve at 390 nm.

## RESULTS

**Steady-State Kinetics.** Previous initial velocity kinetic studies indicate that MCR follows a ternary complex mechanism with methyl-SCoM and CoBSH (11, 12). A rigorous way to distinguish between ping-pong and ternary-complex mechanisms is to hold the concentration of one substrate at a concentration well below its  $K_m$  value and determine an apparent  $V_{max}/K_m$  ( $V/K$ ) at varying concentrations of the other substrate by first-order kinetics. The entire progress curve is followed, and the data are fit to the integrated form of the Michaelis–Menten equation as described in Materials and Methods. In agreement with a ternary-complex mechanism, the apparent  $V/K$  for methyl-SCoM increases in a hyperbolic manner with increasing CoBSH concentrations (Figure 2). In contrast, for a standard ping-pong mechanism, the  $V/K$  for methyl-SCoM would be independent of the concentration of CoBSH. These results appear to contradict the type 2 mechanisms, in which CoBSH binds after methane is formed. The value of  $k_{cat}/K_m$  for methyl-SCoM (at saturating CoBSH) is 18.8  $\text{mM}^{-1} \text{s}^{-1}$  and the  $K_m$  for CoBSH is 0.49 mM. These parameters are consistent with previously determined values.<sup>2</sup> Correcting to 100% active enzyme, based on the spin concentration, the  $k_{cat}/K_m$  for methyl-SCoM would be  $\sim 40 \text{ mM}^{-1} \text{s}^{-1}$ .

Reaction conditions were optimized before undertaking pre-steady-state kinetic studies. The MCR assay mixture for steady-state reactions contains hydroxocobalamin, which stimulates the MCR reaction by recycling CoBSH from

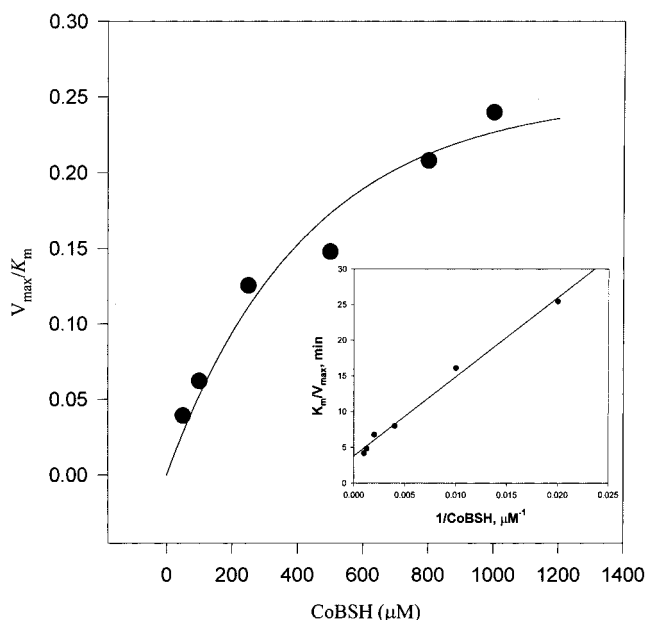


FIGURE 2: Dependence of apparent  $V/K$  for methyl-SCoM on CoBSH concentration. The activity of MCR (34  $\mu$ g) was measured in the presence of methyl-SCoM (100  $\mu$ M) at varying CoBSH concentrations (25  $\mu$ M to 1 mM) at 65 °C. The  $V/K$  for methyl-SCoM and the  $K_m$  for CoBSH obtained from the hyperbolic fit are  $0.34 \pm 0.05 \text{ min}^{-1}$  and  $490 \pm 150 \text{ } \mu\text{M}$ , respectively. Inset: The double reciprocal plot. The value of  $V/K$  for methyl-SCoM, from the reciprocal of the y-intercept is  $0.26 \text{ min}^{-1}$ , which is equivalent to  $19 \text{ mM}^{-1} \text{s}^{-1}$ . The  $K_i$  for methyl-SCoM, from the reciprocal of the x-intercept, is 290  $\mu$ M.

CoBS-SCoM (26). CoBS-SCoM is a strong product inhibitor, with an apparent inhibition constant of 0.6 mM (11). Adding Ti(III)citrate and hydroxocobalamin to the reaction mixture allows one to use CoBS-SCoB as substrate, since cob(I)-alamin catalyzes rapid reduction of the disulfide bonds of CoBS-SCoB, CoBS-SCoM, and CoMS-SCoM (26, 27). The steady-state rate of methane formation is dependent on the concentration of Ti(III)-reduced hydroxocobalamin at sub-saturating methyl-SCoM and saturating concentrations of CoBS-SCoB (Figure 3), with the highest specific activity obtained at 1 mM hydroxocobalamin. At low concentrations of hydroxocobalamin, the reaction rate appears to be limited by product (CoBS-SCoM) dissociation. The calculated maximum specific activity at saturating concentrations of methyl-SCoM is 17 U/mg at 60 °C and, correcting to 100% active MCR<sub>red1</sub>, is approximately 70 U/mg. Therefore, most pre-steady-state experiments using CoBS-SCoB as substrate were performed in the presence of 1 mM hydroxocobalamin. Single turnover reactions using freshly prepared reduced CoBSH could be performed in the absence of cobalamin since very low amounts of product are formed relative to the concentration of saturating substrate.

Since reductive activation of MCR is required for catalysis (6), it seemed feasible that Co(I) could also function by

<sup>2</sup> The previously determined values for the apparent  $K_m$  for methyl-SCoM ranges from 0.6 to 4 mM for methyl-SCoM (11, 12). Thauer published a specific activity, correcting to 1.0 spin/mol of enzyme, for activated MCR of 100 U  $\text{mg}^{-1}$  (250  $\text{s}^{-1}$ ) (6); using this value and a  $K_m$  for methyl-SCoM determined here of  $5.4 \pm 0.3 \text{ mM}$ , the  $k_{cat}/K_m$  is  $50 \text{ mM}^{-1} \text{s}^{-1}$  at 60 °C. Since the enzyme used in our experiments had a  $k_{cat}$  of  $50 \text{ s}^{-1}$ , the corresponding  $k_{cat}/K_m$  would be approximately  $10 \text{ mM}^{-1} \text{s}^{-1}$ . Correcting to 100% active enzyme, based on the spin concentration, the  $k_{cat}/K_m$  would be  $\sim 40 \text{ mM}^{-1} \text{s}^{-1}$ .

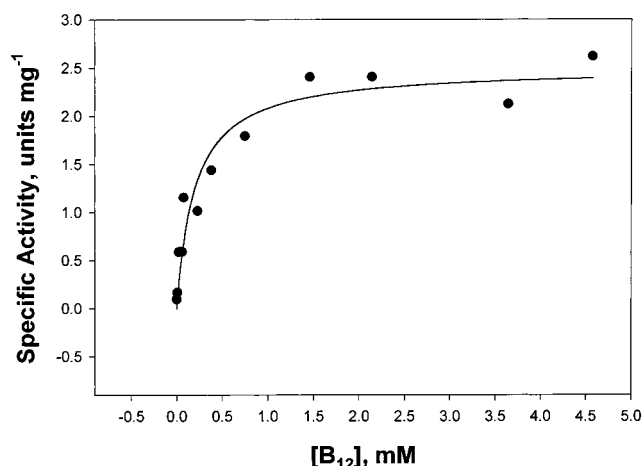


FIGURE 3: Effect of hydroxocobalamin on the steady-state rate with CoBS-SCoB as substrate. The data were fitted with hyperbolic saturation equation.  $V_{\max}$  and  $K_m$  for hydroxocobalamin is  $2.5 \pm 0.2$  U/mg and  $0.20 \pm 0.06$  mM, respectively. The reaction was performed at 60 °C in an assay mixture containing: 1.5 mM CoBS-SCoB, 15 mM TiCitrate, 1 M MOPS (pH 7.0), 0.7 mM methyl-SCoM, and varying amounts of hydroxocobalamin. At saturating concentrations of methyl-CoM, the specific activity would be 17 U/mg at 60 °C.

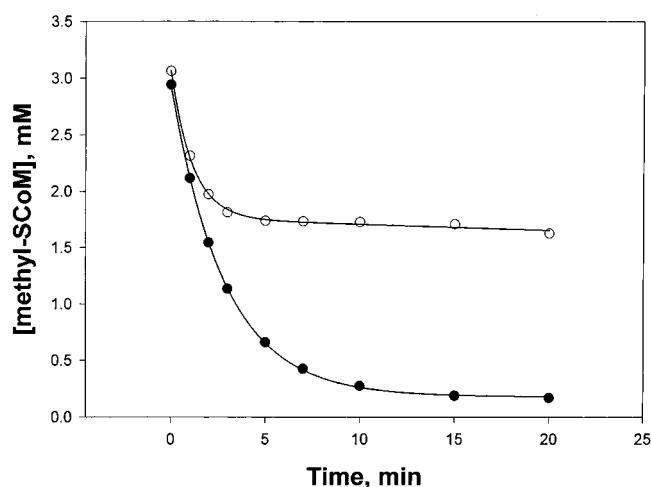


FIGURE 4: The effect of hydroxocobalamin on the steady-state rate of methane formation with 2.0 mM CoBSH as substrate. In the presence (●) and absence (○) of 1.18 mM of hydroxocobalamin, the specific activity based on the initial velocity was 22 U/mg.

activating the enzyme, for example, by increasing the amount of MCR<sub>red1</sub>. However, the *initial velocity* of methane formation with CoBSH (not CoBS-SCoB), as substrate in the absence of hydroxocobalamin is the same as in its presence (Figure 4). Furthermore, the steady-state rate of methane formation with CoBS-SCoB and Ti(III)-reduced hydroxocobalamin is nearly identical to that using CoBSH (not shown, Supplemental Figure 1). Therefore, cobalamin does not appear to have any direct stimulatory effect on MCR. Cobalamin does affect the total amount of product formed (Figure 4). In the presence of hydroxocobalamin, all of the methyl-CoM is converted to methane, even at limiting CoBSH concentrations. On the other hand, in the absence of hydroxocobalamin, less than half of the methyl-CoM is utilized. These results indicate that Co(I) does not directly activate MCR. Its catalytic effect is to reduce the disulfide bond of CoBS-SCoM, the product of the MCR reaction,

which prevents its strong product inhibition and recycles CoBSH for the next catalytic cycle.

**Pre-Steady-State Kinetics.** To monitor as much of the MCR reaction time course as possible, rapid reaction kinetic experiments were performed at 20 °C instead of at the optimum growth temperature (65 °C), where most steady-state reactions have been performed. To compare the steady-state and presteady-state kinetic parameters, we performed some steady-state kinetic experiments at 20 °C. Under normal assay conditions, the specific activity of MCR at 20 °C was 1.0 U/mg, which is 20-fold lower than the activity measured at 65 °C (20 U/mg,  $k_{\text{cat}} = 50 \text{ s}^{-1}$ , assuming a molecular mass of 150 kDa). The MCR 1 isoenzyme used in the rapid reaction studies exhibited a  $K_m$  value for methyl-SCoM of 5.4 mM and a specific activity of 100 U/mg at 60 °C, when corrected for spin concentration. A fairly broad range of  $K_m$  values have been measured previously for the two substrates, from 0.6 to 4 mM for methyl-SCoM and from 0.1 to 0.3 mM for CoBSH (11, 12). We also lowered the Ti(III) citrate concentrations to 1 mM for rapid reaction studies; at this concentration, the specific activity of MCR is 0.6 U/mg and 10 U/mg at 20 and 65 °C, respectively (not shown, Supplemental Figure 2).

To determine whether MCR follows a class 1 or 2 mechanism (above), we performed rapid chemical quench studies by reacting  $^{14}\text{CH}_3\text{-SCoM}$  with MCR<sub>red1</sub> without adding CoBSH. The reaction is acid quenched, and the amount of radioactivity remaining in solution is determined by liquid scintillation counting. Control experiments have demonstrated that the same results are obtained whether methane formation or methyl-SCoM decay is measured since methane is insoluble and is released from solution. However, measuring methane formation in chemical quench reactions is extremely difficult; it is much more convenient to measure methyl-SCoM decay. Furthermore, since the acid quench would convert any putative methyl-Ni intermediates to methane, this method has the potential of measuring C–S bond cleavage, not only methane formation.

When MCR<sub>red1</sub> is rapidly reacted with methyl-CoM without adding CoBSH, methane is formed (Figure 5). The results of these chemical quench studies are consistent with the class 2 mechanism or with the presence of tightly bound CoBSH remaining after MCR is purified to homogeneity. When we analyzed four separate preparations of purified enzyme, we found CoBSH was always present; the average amount of CoBSH present in the purified enzyme is 0.5 ( $\pm 0.1$ ) mol/mol of MCR. We have not yet observed a preparation completely lacking CoBSH. For one preparation of MCR, five separate analyses gave 0.3–0.4 mol of CoBSH/mol of MCR.

Ideally, one would like to perform these reactions with enzyme totally lacking CoBSH; however, as described above, we have been so far been unable to obtain such an enzyme except by incubating with CoBSH analogues (described below). Although steady-state kinetics would not be able to distinguish the two mechanisms, the prediction for the amount of methane formed by MCR (containing bound CoBSH) in single turnover reactions according to the two contrasting mechanisms is quite different. According to the class 2 mechanism, all of the *active* enzyme (equivalent to the amount of red1) would yield methane in the first turnover, plus ~50% of the enzyme (which undergoes activation by

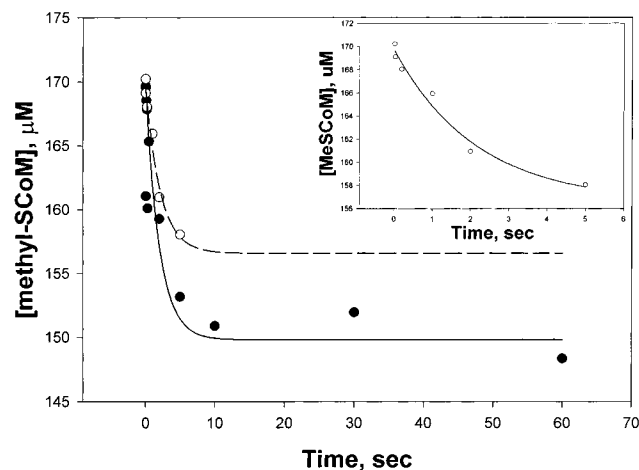


FIGURE 5: Rapid reaction kinetics of MCR with  $^{14}\text{CH}_3\text{-SCoM}$  in the presence and absence of CoBSH.  $26\ \mu\text{M}$  MCR<sub>red1</sub> (1 M Tris-HCl buffer, pH 7.6) in the absence (○) and presence of external  $7.3\ \mu\text{M}$  CoBSH (●) was rapidly mixed with  $170\ \mu\text{M}$   $^{14}\text{CH}_3\text{-SCoM}$  (1 M Tris-HCl buffer, pH 7.6) at  $20\ ^\circ\text{C}$ . The rate constants,  $0.46 \pm 0.15\ \text{s}^{-1}$  (○) and  $0.50 \pm 0.25\ \text{s}^{-1}$  for (●), and the amplitudes,  $13 \pm 2\ \mu\text{M}$  for (○) and  $20 \pm 3\ \mu\text{M}$  for (●), were determined by fitting the data to single-exponential equations. The inset shows the early time points for the reaction without external CoBSH.

the bound CoBSH) would yield methane in the second turnover. According to mechanism 1, only the enzyme containing bound CoBSH would be active in the first turnover. When MCR is reacted with methyl-SCoM at an equimolar stoichiometry (Figure 8B, below) or at 6.5-fold molar excess (Figure 5), the amount of methane formed equals the amount of bound CoBSH. Adding 0.3 molar equiv (relative to MCR<sub>red1</sub>) of CoBSH leads to the formation of 0.3 equiv more methane (Figure 5). Interestingly, the amount of methane formed in the “CoBSH-independent” reaction varies from preparation to preparation, but it is always less than the concentration of active MCR<sub>red1</sub>. These results strongly indicate that MCR requires CoBSH for even a single turnover of methane formation. These results are consistent with mechanism 1 and inconsistent with mechanism 2.

It is important to determine if the rate constants for the experiment shown in Figure 5 ( $0.46\ \text{s}^{-1}$ ) (performed without adding CoBSH) are catalytically relevant. The single-turnover reaction requires the MCR<sub>red1</sub> form of the enzyme; with the MCR-Ni(II), MCR<sub>ox1</sub>, or MCR<sub>ox2</sub> forms, no decrease in the amount of  $^{14}\text{C}$ -labeled  $\text{CH}_3\text{-SCoM}$  is observed. The ratio of  $k_{\text{obs}}/(\text{methyl-CoM concentration})$  for the reaction in the absence of CoBSH is  $5.3\ \text{mM}^{-1}\ \text{s}^{-1}$  at  $20\ ^\circ\text{C}$ , which is significantly higher than the  $k_{\text{cat}}/K_m$  under steady-state conditions ( $0.65\ \text{mM}^{-1}\ \text{s}^{-1}$  at  $20\ ^\circ\text{C}$ ). To compare these rate constants with the steady-state  $k_{\text{cat}}$  ( $50\ \text{s}^{-1}$ ), corrections should be made for Ti(III) citrate, temperature, and the methyl-SCoM concentration. Multiplying the  $k_{\text{obs}}$  values by the  $k_{\text{cat}}$  ratios at 25 and  $65\ ^\circ\text{C}$  equates to 2 and  $9\ \text{s}^{-1}$  at  $65\ ^\circ\text{C}$ . The value of  $k_{\text{obs}}$  shows a hyperbolic dependence on methyl-SCoM concentration. At saturating methyl-SCoM concentrations,<sup>3</sup> these rate constants would be 287 and  $220\ \text{s}^{-1}$ , which is similar to the maximum  $k_{\text{cat}}$  described earlier ( $\sim 250\ \text{s}^{-1}$ ) (6) and here for the enzyme used in these studies ( $250\ \text{s}^{-1}$ ). Therefore, these rate constants for the “CoBSH-independent” reaction are catalytically relevant by the criteria of being as large as the steady-state values of  $k_{\text{cat}}$  and  $k_{\text{cat}}/K_m$ . A 2-fold increase could be applied to account for the Ti(III)citrate

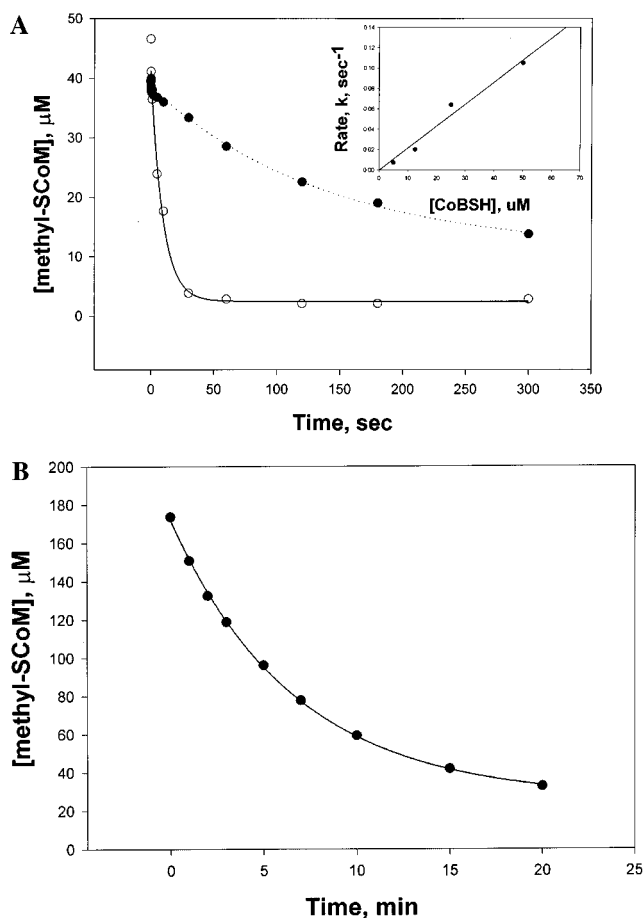


FIGURE 6: Dependence of the observed rate constant on CoBSH concentration. (A) MCR<sub>red1</sub> ( $2\ \mu\text{M}$ ) was preincubated with various concentrations of CoBS-SCoB in the presence of 1 mM hydroxocobalamin at  $20\ ^\circ\text{C}$  before mixing with  $100\ \mu\text{M}$  methyl-SCoM ( $50\ \mu\text{M}$ , final). The rate constants for different concentrations of CoBSH were determined from theoretical single-exponential fits. Representative data are shown for  $5\ \mu\text{M}$  (●) and  $50\ \mu\text{M}$  (○) CoBSH. The second-order rate constant is determined to be  $2.2\ \text{mM}^{-1}\ \text{s}^{-1}$ , as shown in the inset. (B) Slow steady-state turnover in the presence of cobalamin and the absence of CoBSH. MCR<sub>red1</sub> (final concentration  $6.0\ \mu\text{M}$ ) was added to a solution containing 1.3 mM hydroxocobalamin, 5.8 mM Ti(III) citrate,  $180\ \mu\text{M}$  methyl-SCoM, and 1 M Tris-HCl (pH 7.2) (final concentrations) at  $20\ ^\circ\text{C}$  in the absence of CoBSH. The data were fit with a theoretical single-exponential decay. The initial velocity is  $4.3\ \text{min}^{-1}$ , which is equivalent to  $0.03\ \text{U/mg}$ . In the absence of both hydroxocobalamin and CoBSH, the initial velocity is even slower, approximately  $0.002\ \text{U/mg}$ .

concentration, which would make the rate constant about 2-fold higher than the steady-state  $k_{\text{cat}}$ .

If CoBSH is involved in steps leading to cleavage of the C–S bond of methyl-SCoM, the methyl-SCoM decay rate constant would depend on the CoBSH concentration. We performed rapid chemical quench experiments at  $20\ ^\circ\text{C}$  under single turnover conditions for methyl-SCoM in the presence of 2- to 25-fold molar excess of CoBSH (as compared to MCR<sub>red1</sub> concentration). Under these conditions, the rate constant for methane formation strongly depends on the CoBSH concentration (Figure 6A), indicating that CoBSH is required for methane formation. The results are consistent with CoBSH involvement in the rate-limiting step(s) of C–S bond cleavage. Furthermore, when MCR<sub>red1</sub> is reacted with methyl-SCoM in the presence of reduced cobalamin, but without adding CoBSH, methane is formed very slowly



(Figure 6B). Under these conditions, the amount of  $\text{MCR}_{\text{red1}}$  is too low to observe the first turnover. We interpret these results to indicate that the product  $\text{CoMS-SCoB}$  is reduced to  $\text{CoMSH}$  and  $\text{CoBSH}$ , allowing  $\text{CoBSH}$  to re-enter the catalytic cycle. The rate is low because the concentration of  $\text{CoBSH}$  ( $\sim 3 \mu\text{M}$ , based on the ratio of 0.5 mol/mol, above) is well-below its  $K_m$ . In the absence of cobalamin,  $\text{Ti(III)}$  alone can catalyze an extremely low rate of  $\text{CoBS-SCoM}$  reduction (approximately 0.002 U/mg).

Although the above experiments were performed with MCR containing substoichiometric amounts of  $\text{CoBSH}$ , the results strongly indicate that MCR-catalyzed methane formation requires  $\text{CoBSH}$  for even a single turnover of methane formation. In these reactions, methane is formed at catalytically relevant rates in amounts equaling the amount of  $\text{CoBSH}$  present in the reaction mixture. These results are consistent with mechanism 1 and inconsistent with mechanism 2.

**Single Turnover Reactions Using a  $\text{CoBSH}$  Analogue.** One concern of above experiments is that  $\text{CoBSH}$  remains bound to MCR after it has been purified to homogeneity. We found that we can replace  $\text{CoBSH}$  with mercaptohexanoylthreonine phosphate ( $\text{CoB}_6\text{SH}$ ), which contains a six- instead of a seven-carbon alkane chain. This analogue was earlier characterized as an inhibitor and a slow alternative substrate (11). When reacted with MCR in the standard assay with methyl- $\text{SCoM}$  at  $60^\circ\text{C}$ , the steady-state  $k_{\text{cat}}$  is  $4.2 \text{ min}^{-1}$ , which is 1070-fold lower than with  $\text{CoBSH}$  (Figure 7). The steady-state results do not provide evidence to support either mechanism 1 or 2, because the steady-state rate is governed by whatever step is rate limiting in the overall catalytic cycle. When MCR is preincubated with saturating levels of  $\text{CoB}_6\text{SH}$  and reacted with substoichiometric amounts of methyl- $\text{SCoM}$  (i.e., under single turnover conditions for methyl- $\text{SCoM}$ ) at  $20^\circ\text{C}$ , a single-exponential decay curve is observed with a rate constant of  $0.056 \text{ min}^{-1}$  (Figure 8A). This rate is approximately 440-fold lower than that measured under similar conditions with  $\text{CoBSH}$  (Figure 8B). These results sharply contrast with the prediction based on mechanisms such as mechanism 2 in which  $\text{CoBSH}$  is involved in steps succeeding methane formation, where one would expect to observe a decay curve with the same rate constant as with  $\text{CoBSH}$ . The combined results of the steady-state, pre-steady-state, and single-turnover kinetic studies strongly indicate that  $\text{CoBSH}$  is required for a single turnover of methane formation.

## DISCUSSION

There are many unresolved questions related to the mechanism of methane formation by MCR. What is the role of  $\text{CoBSH}$  in the reaction? Can methane be formed by the reaction of the methyl donor (methyl- $\text{SCoM}$ ) directly with

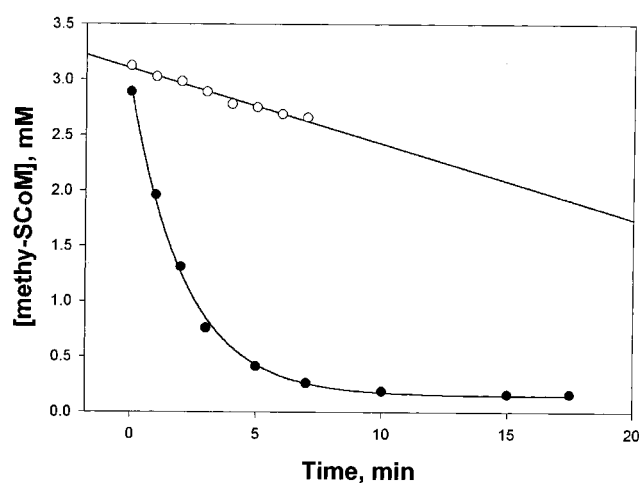


FIGURE 7: Steady-state reaction with 6-mercaptohexanoylthreonine phosphate ( $\text{CoB}_6\text{SH}$ ) (●) or  $\text{CoBSH}$  (○) under saturating conditions. For the reaction with  $\text{CoB}_6\text{SH}$ , the reaction mixture contained 1 M Tris-HCl (pH 7.2), 2.9 mM methyl- $\text{SCoM}$ , 1.7 mM hydroxocobalamin, 1.9 mM  $\text{CoB}_6\text{SH}$ , and 1.3 mg  $\text{MCR}_{\text{red1}}$  in. For the reaction with  $\text{CoBSH}$ , the mixture contained 1 M Tris-HCl (pH 7.2), 3.1 mM methyl- $\text{SCoM}$ , 1.7 mM hydroxocobalamin, 1.7 mM  $\text{CoBSH}$ , and 26  $\mu\text{g}$  of  $\text{MCR}_{\text{red1}}$ . The reaction was started with enzyme and was performed at  $60^\circ\text{C}$ . The rate ( $4.2 \text{ min}^{-1}$ ) for  $\text{CoB}_6\text{SH}$  was determined from linear regression. The initial velocity with  $\text{CoBSH}$  is  $4500 \text{ min}^{-1}$ .

the active form of MCR? Or does the methyl group require prior activation? Is there a methyl-nickel intermediate in the reaction? Does the reaction involve sulfur or methyl radicals? The experiments described here were designed to provide insight into these questions. We used steady-state and rapid kinetics experiments to discriminate between two classes of mechanisms (Figure 1). The first class includes mechanisms in which  $\text{CoBSH}$  is integrally involved in C–S bond cleavage. The Berkessel mechanism is in this class (17). The second class includes mechanisms in which MCR reacts with methyl- $\text{SCoM}$  to form a methyl-nickel intermediate that undergoes protonolysis to form methane before  $\text{CoBSH}$  reacts with the enzyme. Among other rationales for this proposal, Grabarse et al. (16) point out that the MCR reaction bears some similarity with that of ribonucleotide reductase in which a thiyl radical reacts with a thiolate to form a disulfide anion radical.

The experiments described here focus on determining whether  $\text{CoBSH}$  is required to cleave the C–S bond of methyl- $\text{SCoM}$ . Steady-state experiments using first-order kinetics at very low methyl- $\text{SCoM}$  concentrations ( $V/K$  conditions) show that the  $V/K$  for methyl- $\text{SCoM}$  depends on the  $\text{CoBSH}$  concentration. These results concur with the previous steady-state results indicating that the reaction follows a ternary complex mechanism (11, 12). The results also indicate that  $\text{CoBSH}$  must bind before the first irreversible step involving methyl- $\text{SCoM}$ , which presumably is methane release, since transfer of the methyl group from sulfur (methyl- $\text{SCoM}$  or the methylsulfuranyl radical, Figure 1) to  $\text{Ni(I)}$  is expected to be reversible. These results appear to be inconsistent with type 2 mechanisms, in which  $\text{CoBSH}$  binds after methane is formed. However, there still remain caveats with conclusions derived from steady-state kinetics alone. For example, MCR could use a modified ping-pong mechanism in which  $\text{CoBSH}$  binds after the C–S bond is broken and even after methane is made but before methane

<sup>3</sup> The reactions were performed at sub-saturating levels of methyl- $\text{SCoM}$  because at high concentrations of methyl- $\text{SCoM}$ , it is difficult to accurately measure the small decreases in concentration of radioactive substrate. It would be virtually impossible to quantify the pre-steady-state phase of reactions at 40 mM methyl- $\text{SCoM}$  (8-fold greater than  $K_m$ ). However, since the  $\text{CoBSH}$  concentrations are well below those of methyl- $\text{CoM}$  and since the  $k_{\text{obs}}$  value follows a saturation curve similar to that of initial velocity, one can approximate the  $k_{\text{obs}}$  value at saturating methyl- $\text{CoM}$  concentrations by multiplying by the ratio of ( $K_m + s$ )/ $s$ .

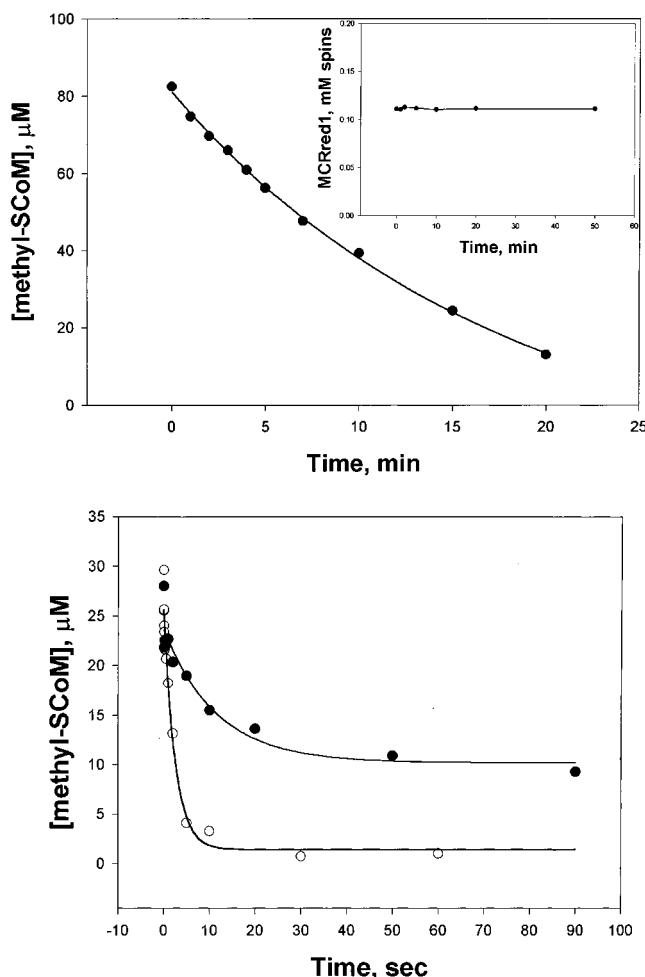


FIGURE 8: Single turnover reactions of MCR with methyl-SCoM and either  $\text{CoB}_6\text{SH}$  or  $\text{CoBSH}$ . (A) Limiting methyl-SCoM and saturating  $\text{CoB}_6\text{SH}$ . The reaction mixture contained  $110\ \mu\text{M}$   $\text{MCR}_{\text{red1}}$  and  $1.5\ \text{mM}$   $\text{CoB}_6\text{SH}$  in  $1\ \text{M}$  Tris-HCl (pH 7.2). The reaction was started by injecting  $83\ \mu\text{M}$   $^{14}\text{CH}_3\text{-SCoM}$  (final concentration). The temperature was  $20\ ^\circ\text{C}$ . The data were fitted with a single-exponential equation ( $k_{\text{obs}} = 0.056 \pm 0.005\ \text{min}^{-1}$ ). The inset shows that the  $\text{MCR}_{\text{red1}}$  spin concentration does not change during the reaction. (B) Reactions of MCR with  $\text{CoBSH}$  and methyl-SCoM under single turnover conditions.  $\text{MCR}_{\text{red1}}$  ( $3.3\ \text{nmol}$ ,  $25\ \mu\text{M}$  red1) was rapidly mixed with  $^{14}\text{CH}_3\text{-SCoM}$  ( $3.7\ \text{nmol}$ ,  $28\ \mu\text{M}$ ) at  $20\ ^\circ\text{C}$  in the absence of  $\text{CoBSH}$  (●), i.e.,  $\text{CoBSH}$  is limiting; and the presence of  $1\ \text{mM}$  external  $\text{CoBSH}$  (○), i.e., methyl-SCoM is limiting. The reaction was followed by monitoring the loss of  $^{14}\text{C}$ -label. The reaction rate was fit to a theoretical single-exponential decay. The rate constant determined from this fit is  $k = 0.09 \pm 0.03\ \text{s}^{-1}$  and the amplitude is  $13 \pm 1\ \mu\text{M}$  ( $0.53\ \text{mol}$  of methane/mol  $\text{MCR}_{\text{red1}}$ ) for the absence of external  $\text{CoBSH}$ . In the presence of external  $\text{CoBSH}$ , the rate constant is  $0.40 \pm 0.06\ \text{s}^{-1}$ .

dissociates. Another complication is that  $\text{CoBSH}$  has been proposed to donate the proton for protonolysis of the methyl-nickel intermediate to form methane, possibly through a proton relay involving two tyrosine residues ( $\beta 367$  and  $\alpha 333$ ) in the active site (13). Furthermore, it is possible that  $\text{CoBSH}$  is required for a conformational change that could be required before methane can be formed (16).

Pre-steady-state kinetic studies have the ability to monitor discrete steps in the MCR reaction mechanism. In the first-described pre-steady-state kinetic studies of MCR, we have focused on the steps preceding methane formation, e.g., C–S bond cleavage, and clarified the role of  $\text{CoBSH}$  in these steps.

It appears relatively straightforward to use pre-steady-state kinetics to distinguish between the class 1 and class 2 mechanisms and discern whether the role of  $\text{CoBSH}$  is to simply regenerate the active  $\text{Ni(I)}$  state of MCR or to play a direct role in C–S bond cleavage or methane formation.

We measured the loss of the  $^{14}\text{C}$ -methyl group of methyl-SCoM as methane by mixing  $^{14}\text{C}$ -methyl-SCoM with  $\text{MCR}_{\text{red1}}$  and rapidly quenching the reaction in acid. Ironically, our first analyses of this reaction under single-turnover conditions indicated that  $\text{CoBSH}$  is not required for methane formation. However, we discovered that MCR contains bound  $\text{CoBSH}$ , even after the enzyme is purified to apparent homogeneity. There is prior evidence for tightly bound  $\text{CoBSH}$  in MCR. In X-ray crystallographic studies (13),  $\text{CoBSH}$  was found in the active site of  $\text{MCR}_{\text{ox1}}$ , even though it was not added to the crystallization solution. In our pre-steady-state reactions performed without adding  $\text{CoBSH}$ , a single exponential decay of methyl-SCoM is observed with amplitude that equals the amount of  $\text{CoBSH}$  remaining bound to the enzyme. If the reaction follows the class 2 mechanism, all of the active enzyme should be capable of producing methane in the first turnover; the bound  $\text{CoBSH}$  would partially regenerate the active enzyme, and that fraction of active enzyme would undergo a second turnover. In contrast, the amount of methane formed equals the amount of active enzyme containing bound  $\text{CoBSH}$ , which is inconsistent with mechanistic class 2 and consistent with class 1 mechanisms. In addition, when rapid kinetic studies are performed under single-turnover conditions for methyl-SCoM, the rate constant for methyl-SCoM decay is dependent upon the  $\text{CoBSH}$  concentration, indicating that  $\text{CoBSH}$  (or a derivative thereof) is involved in the rate-limiting step leading up to C–S bond formation.

What is the rate-limiting step in steady-state turnover? At saturating methyl-SCoM concentrations, the rate constant for methane formation is similar to the maximum  $k_{\text{cat}}$  described earlier ( $\sim 250\ \text{s}^{-1}$ ) (6) indicating that, under these conditions, steady-state turnover is limited by a step(s) preceding or including C–S bond cleavage. The second-order rate constant ( $k_{\text{obs}}/[\text{CoBSH}]$ ) is  $5.3\ \text{mM}^{-1}\ \text{s}^{-1}$  at  $20\ ^\circ\text{C}$ , which is significantly higher than the  $k_{\text{cat}}/K_m$  ( $0.65\ \text{mM}^{-1}\ \text{s}^{-1}$  at  $20\ ^\circ\text{C}$ ), indicating that at low substrate concentrations (under  $V/K$  conditions), a step following C–S bond cleavage is rate limiting in steady-state turnover.

The above results favor the class 1 mechanism for methane formation and are inconsistent with mechanistic class 2; however, it would have been much more straightforward to test the  $\text{CoBSH}$  requirement for methane formation if  $\text{CoBSH}$ -free enzyme had been available for single turnover studies. To allay any remaining concern that it might be the  $\text{CoBSH}$ -free enzyme that reacts with methyl-SCoM in the first turnover, experiments were performed in which the bound  $\text{CoBSH}$  (mercaptoHEPTanoylthreonine phosphate) is removed by preincubating MCR with a  $\text{CoBSH}$  analogue, mercaptoHEXanoylthreonine phosphate ( $\text{CoB}_6\text{SH}$ ).  $\text{CoB}_6\text{SH}$  is a very slow substrate in steady-state turnover, yielding a  $k_{\text{cat}}$  approximately 1000-fold slower than  $\text{CoBSH}$ . Reaction of MCR in a saturating solution of  $\text{CoB}_6\text{SH}$  with stoichiometric levels of methyl-SCoM under single turnover conditions yields a single-exponential decay with a rate constant for methane formation that is 440-fold slower than with  $\text{CoBSH}$ . There is no observable phase of methane



formation at the rapid rate observed in similar reactions performed in the absence or presence of CoBSH. These results are inconsistent with mechanism 2, which predicts that the first turnover of methane formation should occur at the same rate with CoBSH or CoB<sub>6</sub>SH. In agreement with mechanism 1, MCR absolutely requires the slow substrate analogue to form methane, even when the rate of methanogenesis is decreased by 10<sup>3</sup>-fold. The implications of such a tight coupling between the reaction with CoBSH or its analogue and methane formation is discussed below.

The combined results strongly indicate that CoBSH is required for a single turnover of methane formation. How might CoBSH be involved in methane formation? One possibility is that CoBSH is required to donate the proton that results in lysis of the methyl–Ni bond (13). It was suggested that this proton transfer is assisted by tyrosine residues  $\beta$ 367 and  $\alpha$ 333. Our chemical quench experiments were designed with an acid quench to promote the direct cleavage of any acid labile intermediate, like the methyl–Ni species, en route to methane formation. Furthermore, it is unreasonable to suspect that any proton-transfer reaction could be rate limiting in a reaction with a half time of 12 min (with CoB<sub>6</sub>SH). Therefore, we conclude that, even if CoBSH is involved in proton transfer, this would not account for the CoBSH requirement that is observed in the chemical quench reaction.

Another possible role for CoBSH is to induce a conformational change in MCR that is required for methane formation. There is indeed evidence for a substrate-induced conformational change in MCR (16). However, could this be the origin of the strict requirement of CoBSH for methane formation? Could CoBSH be required for one turnover of methane formation without participating directly in C–S bond cleavage? The experiments with CoB<sub>6</sub>SH provide a test of this hypothesis. Given the strong structural similarity, we assume that CoB<sub>6</sub>SH would elicit the same conformational change in MCR as CoBSH. In both the steady-state and pre-steady-state reactions, CoB<sub>6</sub>SH becomes a required substrate. The rate of methane formation is 1000-fold slower in the steady-state and 440-fold slower in the pre-steady-state reaction relative to the reaction with CoBSH. We consider that a substrate-induced conformational change may indeed promote catalysis. However, such a CoBSH-induced conformational change would not explain the strict requirement of CoBSH (or its 6-carbon analog) for methane formation or how CoBSH or CoB<sub>6</sub>SH would participate in the rate-limiting step in the methane formation. Assuming that CoB<sub>6</sub>SH would elicit the same conformational change induced by CoBSH and at a similar rate, our results indicate that CoBSH plays an integral role in a rate-limiting step in methane formation. Such a role is consistent with mechanism 1.

What is the rate-limiting chemical step in methane formation in which CoBSH is involved? According to mechanism 1, this step may be either formation of the CoBS<sup>•</sup> radical or adduct formation between CoBS<sup>•</sup> radical and methyl–SCoM, which would promote C–S bond cleavage. There are some drawbacks of mechanism 1. One problem in Figure 1 and in similar mechanisms: how does MCR generate the CoBS<sup>•</sup> thiyl radical? Perhaps the active-site thioglycine residue (the shaded R and R<sup>•</sup> in the mechanism could serve as the electron acceptor. However, the redox potential for the thioglycine/

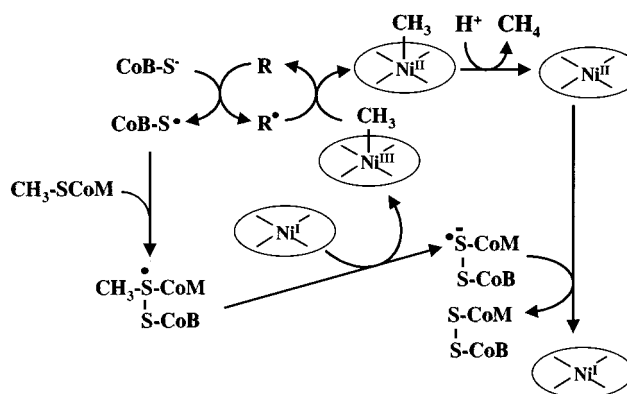


FIGURE 9: Alternative mechanism 1. In this mechanism, a radical species (R), couples formation of the CoBS<sup>•</sup> radical to reduction of CH<sub>3</sub>–Ni(III). The redox potential of the R/R<sup>•</sup> couple should be fairly oxidizing. Generation of a radical by reduction is shown; however, it is also possible that the active enzyme has a yet-uncharacterized radical that is reduced to a diamagnetic RH species by CoBSH and redoxidized back to R<sup>•</sup> by methyl–Ni(III).

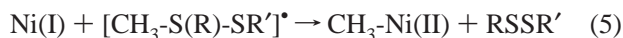
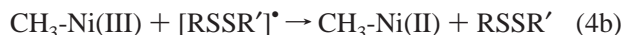
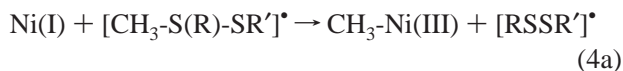
thioketyl anion radical is  $\sim -1.4$  V and that for a thiyl radical/thiol is  $\sim +0.5$  to 1.0 V. Therefore, it is thermodynamically improbable that CoBSH could reduce the thioglycine residue. On the other hand, reduction of Ni(II) to Ni(I) at the end of the catalytic cycle by the thioketyl radical would be thermodynamically favorable.

We propose an alternative to mechanism 1 that alleviates some of the thermodynamic problems associated with mechanism 1 (Figure 9). This mechanism, like the one shown in Figure 1, is similar to some previous proposals (10, 17) and includes a role for a radical (R), which was suggested to be involved in methane formation (16). Although one can conceive of other ways to include CoBSH in the initial steps of methane formation, we consider alternative mechanism 1 as a testable working hypothesis. The first step is generation of the CoBSH radical, CoB–S<sup>•</sup>. A potential problem with this proposal is that the crystal structure indicates that bound CoBSH completely occludes the active site, barring entry of methyl–SCoM. This and other considerations led Grabarse et al. to recently favor a mechanism similar to mechanism 2 in which a proton, possibly from CoBSH, activates methyl–SCoM toward nucleophilic attack by Ni(I) (16). However, although the crystal structure indicates that CoBSH must bind after methyl–CoM, steady-state evidence presented here and elsewhere indicates that no reaction occurs until the ternary complex is formed. Thus, it is possible that methyl–SCoM and then CoBSH bind; then the reaction begins with generation of CoB–S<sup>•</sup>. The radical, “R” could be involved in generating CoB–S<sup>•</sup>. In this alternative mechanism, the redox potential for the R/R<sup>•</sup> couple should be fairly positive since the redox potentials for the methyl–Ni(III)/methyl–Ni(II) and the thiyl radical/thiol couples are above +0.5 V. Then, as first suggested by Berkessel, CoB–S<sup>•</sup> could react with methyl–SCoM to form a sulfuranyl radical. The methyl–S bond would then be more prone to homolytic cleavage by Ni(I) to form methyl–Ni(III) and a disulfide anion radical. The redox potential for the disulfide/disulfide-anion-radical couple ( $< -1.0$  V) is more negative than for the Ni(II)/Ni(I) couple. Therefore, after cleavage of the methyl–Ni(II) bond to form methane, formation of the heterodisulfide product could be linked to reformation of the active Ni(I) state. This proposal would rationalize the requirement of

CoBSH for cleavage of the C–S bond of methyl-SCoM.

Alternative mechanism 1 is consistent with relevant chemical models of MCR-catalyzed methanogenesis. That the Ni(I) form of the pentamethyl ester of F<sub>430</sub> reacts with methyl donors (e.g., methyl iodide, methyl tosylate, methyl dialkyl sulfonium) to yield methane through protonation of a methylnickel intermediate (28–30) suggests that the class 2 mechanism also is feasible. Jaun (31) and Berkessel (17) have suggested mechanisms similar to mechanism 1, in which a methyl sulfuranyl radical intermediate precedes the methylnickel species, because methyl thioethers related to and including the natural substrate, methyl-SCoM, do not react directly with Ni(I)-F<sub>430</sub> (31). Additionally, it was recently demonstrated that a radical pair, consisting of the Ni(I) state of F<sub>430</sub> and a thiyl radical, reacts with a methyl thioether to yield methane and the corresponding disulfide (32), which establishes an important chemical precedent for class 1 mechanisms.

Figure 9 indicates that the reaction between Ni(I) and the methyl-sulfuranyl radical forms methyl-Ni(II) and the heterodisulfide. This reaction could occur by a nucleophilic attack of Ni(I) on the methyl group (eq 4) or by attack of Ni(I) on the equivalent of a methyl radical (eq 5). Equation 5 would likely be favored since eq 4 is spin-forbidden. In addition, the MCR structure indicates that the methyl group of the proposed sulfuranyl radical would be too far from Ni(I) to permit a nucleophilic attack. However, a nucleophilic attack would be more easily reconciled with the stereochemical results (18). Furthermore, methyl-Ni(III) is highly oxidizing, and electron transfer from the disulfide radical anion to methyl-Ni(III) would yield the same final products as in eq 5. To reiterate, there may be some defects in mechanism 1 or its alternative shown in Figure 9, but our results indicate that any reasonable mechanism should include a role for CoBSH in the steps prior to or including methane formation.



Why are the steady-state and single turnover reactions so slow with a CoBSH analogue that is only one methylene group shorter than CoBSH itself? Given the strong structural similarity between CoBSH and CoB<sub>6</sub>SH, it appears unlikely that the observed requirement reflects a structural role, for example, a CoBSH-dependent conformational change, which CoB<sub>6</sub>SH would surely elicit. In the crystal structures of the various Ni(II) states of MCR, whether it is free (ox1-silent) or in a disulfide linkage with coenzyme M (Ni(II)-silent), CoBSH is in a similar position with its phosphate group bound at the upper lip of the 30 Å deep active site well. According to mechanism 1, an analogue that is one methylene group (~1.4 Å) shorter could be less reactive in donating its electron to the putative “R” electron acceptor to form the CoB-S<sup>•</sup> radical. An electron-transfer reaction over a 1.4 Å longer covalently bonded distance would be expected to occur 5-fold slower. However, shortening the alkyl chain of CoBSH would likely leave a through-space gap of 1.4 Å

between the CoB sulfur and the thioglycine, which would significantly magnify the effect. Significant penalties are incurred for each through-space “jump” in an electron-transfer reaction (33). The shorter CoBSH analogue would also probably be at a nonoptimal location in the active site to effectively condense with methyl-SCoM to form the sulfuranyl radical.

In summary, our results are consistent with a role for coenzyme B in a rate-limiting step involved in methane formation. It appears unlikely that this role is explained solely by a CoBSH-induced conformational change or requirement for CoBSH in proton transfer, although these steps could be important in methane formation. We suggest that coenzyme B (perhaps as a radical) forms an adduct with methyl-SCoM and, thereby, promotes C–S bond cleavage. Further studies will be required to detect and characterize the intermediates and the elementary steps in methane synthesis.

## ACKNOWLEDGMENT

We are grateful to Dr. Javier Seravalli for critically reading the manuscript.

## SUPPORTING INFORMATION AVAILABLE

Supplemental Figure 1 compares the steady-state rate using CoBS–SCoB and reduced hydroxocobalamin with that using CoBSH. Supplemental Figure 2 shows the steady-state MCR reaction progress curve under rapid reaction conditions of low (1 mM) Ti(III) citrate and at 20 °C. This material is available free of charge via the Internet at <http://pubs.acs.org>.

## REFERENCES

- DiMarco, A. A., Bobik, T. A., and Wolfe, R. S. (1990) *Annu. Rev. Biochem.* 59, 355.
- Ellermann, J., Kobelt, A., Pfaltz, A., and Thauer, R. K. (1987) *FEBS Lett.* 220, 358–62.
- Diekert, G., Klee, B., and Thauer, R. K. (1980) *Arch. Microbiol.* 124, 103–106.
- Diekert, G., Jaenchen, R., and Thauer, R. K. (1980) *FEBS Lett.* 119, 118–120.
- Whitman, W. B., and Wolfe, R. S. (1980) *Biochem. Biophys. Res. Commun.* 92, 1196–1201.
- Goubeaud, M., Schreiner, G., and Thauer, R. K. (1997) *Eur. J. Biochem.* 243, 110–114.
- Albracht, S. P. J., Ankel-Fuchs, D., Böcher, R., Ellermann, J., Moll, J., van der Zwann, J. W., and Thauer, R. K. (1988) *Biochim. Biophys. Acta* 941, 86–102.
- Rospert, S., Böcher, R., Albracht, S. P. J., and Thauer, R. K. (1991) *FEBS Lett.* 291, 371–375.
- Becker, D. F., and Ragsdale, S. W. (1998) *Biochemistry* 37, 2639–47.
- Thauer, R. K. (1998) *Microbiology UK* 144, 2377–2406.
- Ellermann, J., Hedderich, R., Böcher, R., and Thauer, R. K. (1988) *Eur. J. Biochem.* 172, 669–677.
- Bonacker, L. G., Baudner, S., Mörschel, E., Böcher, R., and Thauer, R. K. (1993) *Eur. J. Biochem.* 217, 587–595.
- Ermler, U., Grabarse, W., Shima, S., Goubeaud, M., and Thauer, R. K. (1997) *Science* 278, 1457–1462.
- Telser, J., Davydov, R., Hornig, Y. C., Ragsdale, S. W., and Hoffman, B. M. (2001) *J. Am. Chem. Soc.* 123, 5853–60.
- Telser, J., Hornig, Y.-C., Becker, D., Hoffman, B., and Ragsdale, S. W. (2000) *J. Am. Chem. Soc.* 122, 182–183.
- Grabarse, W. G., Mählert, F., Duin, E. C., Goubeaud, M., Shima, S., Thauer, R. K., Lamzin, V., and Ermler, U. (2001) *J. Mol. Biol.* 309, 315–330.
- Berkessel, A. (1991) *Bioorg. Chem.* 19, 101–115.

18. Ahn, Y., Krzycki, J. A., and Floss, H. G. (1991) *J. Am. Chem. Soc.* 113, 4700–4701.
19. Gunsalus, R. P., Romesser, J. A., and Wolfe, R. S. (1978) *Biochemistry* 17, 2374–2377.
20. Bobik, T. A., and Wolfe, R. S. (1988) *Proc. Natl. Acad. Sci. U.S.A.* 85, 60–3.
21. Noll, K. M., Donnelly, M. I., and Wolfe, R. S. (1987) *J. Biol. Chem.* 262, 513–515.
22. Noll, K. M., Rinehart, K. L., Jr., Tanner, R. S., and Wolfe, R. S. (1986) *Proc. Natl. Acad. Sci. U.S.A.* 83, 4238–4242.
23. Schönheit, P., Moll, J., and Thauer, R. K. (1980) *Arch. Microbiol.* 127, 59–65.
24. Bradford, M. M. (1976) *Anal. Biochem.* 72, 248–254.
25. Pfaltz, A., Juan, B., Fassler, A., Eschenmoser, A., Jaenchen, R., Gilles, H. H., Diekert, G., and Thauer, R. K. (1982) *Helv. Chim. Acta* 65, 828–865.
26. Rouviere, P. E., Bobik, T. A., and Wolfe, R. S. (1988) *J. Bacteriol.* 170, 3946–52.
27. Hedderich, R., and Thauer, R. K. (1988) *FEBS Lett.* 234, 223–227.
28. Lin, S.-K., and Jaun, B. (1991) *Helv. Chim. Acta* 74, 1725–1738.
29. Lin, S.-K., and Jaun, B. (1992) *Helv. Chim. Acta* 75.
30. Jaun, B., and Pfaltz, A. (1988) *J. Chem. Soc. Chem. Commun.* 1327, 293–294.
31. Jaun, B. (1990) *Helv. Chim. Acta* 73, 2209–2217.
32. Signor, L., Knuppe, C., Hug, R., Schweizer, B., Pfaltz, A., and Jaun, B. (2000) *Chem.-Eur. J.* 6, 3508–3516.
33. Gray, H. B., and Winkler, J. R. (1996) *Annu. Rev. Biochem.* 65, 537–561.

BI011196Y